

# Two-wave-band color-mixing binoculars for the detection of wholesome and unwholesome chicken carcasses: a simulation

Fujian Ding, Yud-Ren Chen, and Kuanglin Chao

Visual inspection of wholesome and unwholesome chicken carcasses with a novel two-narrowband color-mixing technique for optically enhanced binoculars is simulated. From mean spectra of wholesome, airsacculitis (air-sac), cadaver, inflammatory process (IP), septicemia–toxemia (septox), and tumor chicken samples, 10 nm wave-band pairs are selected using color difference and chromaticness difference indices for simulation of multitarget and single-target detection. The color appearance simulation uses the CIECAM97s color appearance model. Results show that for multitarget detection, the wave-band pair of (454 nm, 578 nm) is able to differentiate all six chicken conditions. For single-target detection of wholesome, air-sac, cadaver, and tumor, the wave-band pairs of (449 nm, 571 nm), (441 nm, 576 nm), (458 nm, 576 nm), and (431 nm, 501 nm), respectively, easily distinguish the target condition from the other five conditions. For single-target detection of IP and septox, the wave-band pairs of (454 nm, 591 nm) and (454 nm, 590 nm), respectively, are able to differentiate the target conditions from wholesome and tumor conditions but have difficulty with the other chicken conditions. The two-color-mixing technique shows promise for use in small-scale processing plant environments to improve the visual inspection process.

*OCIS codes:* 330.1730, 330.1880, 330.1400.

## 1. Introduction

In recent years, U.S. consumption of poultry products has increased significantly. To ensure a safe meat supply, U.S. legislation requires that each carcass at poultry slaughter plants be inspected by Food Safety and Inspection Service (FSIS) inspectors of the U.S. Department of Agriculture (USDA).<sup>1</sup> These experienced inspectors visually and manually inspect the carcass exterior, the inner surfaces of the body cavity, and the visceral organs for apparent diseases and defects.

The condition of septicemia–toxemia (septox) is the most common cause for carcass condemnation (removal of a bird from the processing line). Septox

is a systemic disease caused by pathogenic microorganisms or their toxins in the bloodstream. Septox carcasses are often dark red to bluish in color, dehydrated, stunted, or edematous.<sup>2</sup> The other major causes of removal from the processing line are airsacculitis (air-sac, a lung disease), tumor (cartilaginous nodules), cadaver (improper bleeding), and inflammatory process (IP). These unwholesome carcasses demonstrate a variety of color changes.

FSIS has adopted the Hazard Analysis and Critical Control Point (HACCP) system, which requires poultry processors to identify all food safety hazards in their process and to identify critical control points adequate to address these hazards.<sup>3</sup> The HACCP system, together with the demands of increased production, has increased the workload of FSIS plant inspectors. To address poultry safety concerns and meet growing consumer demand, there is an urgent need to develop new inspection technologies. Researchers at the USDA Instrumentation and Sensing Laboratory (ISL) have developed visible–near-infrared (Vis–NIR) spectroscopic methods and multispectral imaging techniques for use in on-line, real-time classification of poultry carcasses in slaughter plants.<sup>4–10</sup> For example, the ISL Vis–NIR poultry inspection system can separate chicken carcasses into wholesome

---

The authors are with the Instrumentation and Sensing Laboratory, Henry A. Wallace Beltsville Agricultural Research Center, Agricultural Research Service, U.S. Department of Agriculture, Building 303 BARC-East, 10300 Baltimore Avenue, Beltsville, Maryland 20705. Y.-R. Chen's e-mail address is [Cheny@ba.ars.usda.gov](mailto:Cheny@ba.ars.usda.gov).

Received 22 September 2004; revised manuscript received 30 March 2005; accepted 22 April 2005.

0003-6935/05/265454-09\$15.00/0

and unwholesome classes with a success rate of 95% at a processing line speed of 91 birds/min.

Vis-NIR spectroscopy has also been used to characterize the spectral intensity variations of wholesome and unwholesome chicken meats.<sup>10</sup> Results have shown that there are at least three prominent bands around 445, 485, and 560 nm in the visible region that can be attributed to three major derivatives of the myoglobin pigment: deoxymyoglobin, metmyoglobin, and oxymyoglobin, respectively. Changes in relative amounts of the three species determine the appearance of meat color, which forms the basis for the classification analysis by Vis-NIR and imaging spectroscopy.

In general, spectral imaging methods for chicken inspection accentuate the analysis of spectral and spatial features but rarely reflect color features as perceived through human vision, for which color appearance is composed of lightness and chromaticness. A color-based optical inspection device might be an alternative to more-complex spectral imaging systems as an aid to inspectors for distinguishing between wholesome and unwholesome chickens.

At ISL, a low-cost optically enhanced device that can assist inspectors or plant processors in small meat and poultry plants (that have fewer than 300 employees) to conduct inspection *in situ* is being developed. The device consists of binoculars equipped with two narrowband optical filters and an active light source. Using a two-color-mixing technique, small plant operators will be able to detect defective, diseased, and contaminated carcasses when viewing through the optical device. Two-band color mixing has been shown to be directly related to the two-color-band ratio criterion,<sup>11</sup> which has been used for successful separation of wholesome and unwholesome chickens.<sup>12</sup>

This paper reports the results of the research (i) to select potential wave-band pairs according to color difference and chromaticness difference indices and (ii) to design optically enhanced binoculars for chicken inspection based on a two-color-mixing technique. The simulation of color appearance is also presented.

## 2. Materials and Methods

### A. Chicken Samples and Vis-NIR Reflectance Spectra

A total of 467 chicken carcasses (213 wholesome, 51 air-sac, 80 cadaver, 51 IP, 64 septox, and 8 tumor) were obtained from a processing line at a poultry slaughter plant in Cordova, Maryland. These wholesome and unwholesome conditions were identified in the plant by USDA FSIS inspectors. Chicken carcasses were marked according to condition and placed in plastic bags to minimize dehydration during transport. Then the bags were placed in coolers, covered with ice, and transported to the ISL facility in Beltsville, Maryland, within 2 h for the experiment.

For each sample, the right breast was removed with the skin intact, and from this a 49 mm diameter circular area was cut out. The skin, approximately

4 mm thick, was removed and set aside while the meat was sliced to a thickness of 15 mm. Before sample reflectance measurements were taken, dark background and white reference (black and white polytetrafluoroethylene, respectively) measurements were collected. To take a sample reflectance measurement, the sample (chicken meat with skin overlaid) was placed in the sample holder and a fiber-optic probe was positioned 2 cm above the surface of the sample.

Vis-NIR reflectance spectra were collected with a photodiode array spectrophotometer (Oriel Co., Stratford, Connecticut) in the wavelength range of 411.0–923.0 nm, in increments of 0.5 nm, resulting in 1024 data points/spectrum. In an effort to improve the signal-to-noise ratio, each spectrum was the average of 244 scans of the diode array, where each scan was a result of a 0.0328 s photodiode array exposure.

### B. Two-Band Color Mixing

The Commission Internationale de l'Éclairage (CIE) tristimulus values  $X$ ,  $Y$ , and  $Z$  of the color of each chicken sample were obtained by multiplying the spectral irradiance of the illumination  $S_\lambda$ ; the reflectance of the chicken sample  $R_\lambda$ ; and the 1931 CIE standard observer functions  $\bar{x}$ ,  $\bar{y}$ , and  $\bar{z}$ :

$$\begin{aligned} X &= k \sum_{\lambda} S_{\lambda} R_{\lambda} \bar{x}_{\lambda}, \\ Y &= k \sum_{\lambda} S_{\lambda} R_{\lambda} \bar{y}_{\lambda}, \\ Z &= k \sum_{\lambda} S_{\lambda} R_{\lambda} \bar{z}_{\lambda}, \end{aligned} \quad (1)$$

where  $k$  is a normalizing constant. In a special case where absolute values for the spectral power distribution are given, it is convenient to use  $k = 683 \text{ lm/W}$ , from which the calculated value of  $Y$  is the luminous flux expressed in lumens.

For color perception with an optical device, the tristimulus values ( $X$ ,  $Y$ , and  $Z$ ) of an object can be defined as

$$\begin{aligned} X &= k \sum_{\lambda} \tau_{\lambda} S_{\lambda} R_{\lambda} \bar{x}_{\lambda}, \\ Y &= k \sum_{\lambda} \tau_{\lambda} S_{\lambda} R_{\lambda} \bar{y}_{\lambda}, \\ Z &= k \sum_{\lambda} \tau_{\lambda} S_{\lambda} R_{\lambda} \bar{z}_{\lambda}, \end{aligned} \quad (2)$$

where  $\tau_{\lambda}$  is the spectral transmittance of the optical device. The tristimulus values of colors are additive.<sup>13</sup> This means that for the mixing of two colors, the tristimulus values  $X_m$ ,  $Y_m$ , and  $Z_m$  of the new color can be calculated from the tristimulus values of the colors being mixed<sup>13</sup>:

$$\begin{aligned}
X_m &= X_1 + X_2, \\
Y_m &= Y_1 + Y_2, \\
Z_m &= Z_1 + Z_2.
\end{aligned}
\tag{3}$$

### C. Design Parameters for Color-Mixing Binoculars

The selection of a pair of wavelengths for chicken inspection with two-color mixing was designed for use on a set of  $8 \times 42$  binoculars. The color difference index  $\Delta E$  and the chromaticness difference index  $\Delta S'$  of wholesome, air-sac, cadaver, IP, septox, and tumor chicken samples in the CIELUV color space were used to determine the potential wavelength pairs. The tristimulus values for 10 nm wave bands centered at  $\lambda_1$  and  $\lambda_2$  were first calculated with Eq. (2) in the visible spectrum (411–721 nm). With Eq. (3), the tristimulus values for color mixing of all the possible pairs of  $\lambda_1$  and  $\lambda_2$  were calculated. These tristimulus values were converted into CIELUV uniform color space values, and values were calculated for both the color difference and the chromaticness difference indices between the chicken sample categories. To some extent, the index  $\Delta S'$  is more suitable for the cases in which the band ratio criterion works.

As seen in Eq. (2), the tristimulus values are a wavelength-by-wavelength product of the illuminant spectral power distribution, the sample reflectance, and the color-matching functions. In this study, the light source is the CIE Standard Illuminant D65 with a correlated color temperature of 6500 K. The filters have a bandwidth (full width at half-maximum) of 10 nm and a transmission of 50%.

Total illuminance from the CIE Source D65 onto the samples was 5000 lx; thus the illuminance  $E_{\lambda_i}$  for each 10 nm wave band centered at  $\lambda_i$  (for  $i = 1, 2$ ) can be calculated as

$$E_{\lambda_i} = \frac{\int_{\lambda_i - \Delta\lambda_i/2}^{\lambda_i + \Delta\lambda_i/2} \tau_\lambda H_\lambda \bar{y}_\lambda d\lambda}{\int_0^\infty H_\lambda \bar{y}_\lambda d\lambda} \times 5000 \text{ lx},
\tag{4}$$

where  $H_\lambda$  is the relative spectral energy distribution factor of the CIE Source D65, and  $\tau_\lambda$  is the spectral transmission of the binoculars.

The CIELUV color coordinates were calculated from the color-mixed tristimulus values as follows<sup>14</sup>:

$$L^* = \begin{cases} 25 \left( \frac{100Y}{Y_n} \right)^{1/3} - 16, & \text{if } \frac{Y}{Y_n} > 0.00856, \\ 903.29 \left( \frac{Y}{Y_n} \right), & \text{otherwise,} \end{cases}$$

$$\begin{aligned}
u^* &= 13L^*(u' - u_n'), \\
v^* &= 13L^*(v' - v_n'),
\end{aligned}
\tag{5}$$

with

$$u' = \frac{4X}{X + 15Y + 3Z},$$

$$v' = \frac{9Y}{X + 15Y + 3Z},$$

$$u_n' = \frac{4X_n}{X_n + 15Y_n + 3Z_n},$$

$$v_n' = \frac{9Y_n}{X_n + 15Y_n + 3Z_n}.$$

The tristimulus values ( $X_n$ ,  $Y_n$ , and  $Z_n$ ) are those of the nominal white reference. In this study, the spectral reflectance of the white reference was set to equal 1.0 for all wavelengths.

The color difference index  $\Delta E$  takes into account the difference in lightness, hue, and saturation between two samples and is calculated as the Euclidean distance between two points in this three-dimensional space<sup>14</sup>:

$$\Delta E(L^*u^*v^*) = [(\Delta L^*)^2 + (\Delta u^*)^2 + (\Delta v^*)^2]^{1/2}. \tag{6}$$

The chromaticness difference index  $\Delta S'$  takes into account the difference in hue and saturation between two samples and is calculated as

$$\Delta S' = 13[(\Delta u')^2 + (\Delta v')^2]^{1/2}. \tag{7}$$

Multitarget detection attempts to identify which category (of the possible six) that a chicken sample belongs to, whereas single-target detection considers one category at a time and decides whether the sample belongs to that category. For multitarget detection, for each possible pair of  $\lambda_1$  and  $\lambda_2$ , the color difference index  $\Delta E$  was calculated between all the categories of chicken conditions for a total of 15 values per wave-band pair. Thus, 15 values were calculated for each of the 90,000 possible wave-band combinations. The chromaticness difference index  $\Delta S'$  was also calculated in this manner.

For single-target detection, a set of  $\Delta E$  values was calculated for each possible pair of  $\lambda_1$  and  $\lambda_2$  for one chicken condition at a time, comparing this category to each of the other five chicken conditions, for a set of five values per wave-band pair per category. Thus, 30 values were calculated for each of the 90,000 possible wave-band combinations. The chromaticness difference index  $\Delta S'$  was also calculated in this manner.

A combination of maximum and minimum operations was used to determine the potential wave-band pairs for multitarget and single-target discrimination of chicken conditions by color difference index  $\Delta E$  and by chromaticness difference index  $\Delta S'$ . For example, 15 values of color difference  $\Delta E$  were calculated for

each of the 90,000 possible wave-band combinations of  $\lambda_1$  and  $\lambda_2$ . For each combination, the minimum operation selected the lowest  $\Delta E$  from among the 15 values. Selecting the smallest difference guarantees that all the categories can be differentiated with this wave-band pair. From the resulting set of 90,000 minimum values, the maximum operation was used to select the wave-band pair with the largest  $\Delta E$  as the potential wave-band pair. This selection process was repeated for detection based on single-target color difference and also for multitarget and single-target chromaticness difference index  $\Delta S'$ .

#### D. Simulation of Color Appearance

Simulation of color appearance was performed on a Sony Trinitron color CRT monitor by use of the revision of CIECAM97s proposed by Fairchild.<sup>15-17</sup> Corrections for chromatic adaptation were needed to simulate binocular viewing conditions on the monitor display.

The color monitor was calibrated and profiled with a GretagMacbeth Eye-One Display (GretagMacbeth, New Windsor, New York). The physical characteristics of this monitor are listed in Table 1. The simulation used the same design parameters as those for the color-mixing binoculars. For the simulation reference white point, the CIE Standard Illuminant D65 was used, and the illumination was measured to be 195.7 lx.

The color display monitor creates different colors by adding mixtures of the three primary colors, red ( $R$ ), green ( $G$ ), and blue ( $B$ ). The transformation from  $(X, Y, Z)$  to  $(R, G, B)$  color space was performed by the following transformation matrix<sup>15-17</sup>:

$$\begin{bmatrix} R \\ G \\ B \end{bmatrix} = M \begin{bmatrix} X \\ Y \\ Z \end{bmatrix}, \quad (8)$$

where  $0 \leq R \leq 1$ ,  $0 \leq G \leq 1$ , and  $0 \leq B \leq 1$ . The transformation matrix  $M$  for the monitor is

$$M = \begin{bmatrix} 0.0485 & -0.0220 & -0.0072 \\ -0.0177 & 0.0323 & 0.0005 \\ 0.0009 & -0.0032 & 0.0169 \end{bmatrix}.$$

The color on the monitor display produced by a

**Table 1. Physical Characteristics of Sony Trinitron Color CRT Monitor**

Maximum luminance	62.28 cd/m <sup>2</sup>
White pixel RGB values	255, 255, 255
CIE( $x, y$ ) chromaticity coordinates of white pixels	0.3112, 0.3295
CIE( $x, y$ ) of the CRT's $R$ primaries	0.6261, 0.3426
CIE( $x, y$ ) of the CRT's $G$ primaries	0.2909, 0.6091
CIE( $x, y$ ) of the CRT's $B$ primaries	0.1479, 0.0698
Gamma: $R$ primaries	2.133
Gamma: $G$ primaries	2.145
Gamma: $B$ primaries	2.117

particular red-green-blue (RGB) specification depends on the gamma characteristics of the display<sup>13,18</sup> and the input voltage for each  $R, G$ , or  $B$  channel. The simulation of using color-mixing binoculars to view chicken samples, taking into account monitor viewing conditions, was used to calculate the RGB specifications needed to display colors on the monitor as if viewed through binoculars. Given the gamma characteristics that were measured for the monitor (listed in Table 1), the input voltages could be calculated from the power function for display intensity,

$$V = \left( \frac{L}{L_{\max}} \right)^{(1/\gamma)}, \quad (9)$$

where  $V$  is the normalized input voltage ( $0 < V < 1$ ) for each  $R, G$ , or  $B$  channel, and  $L_{\max}$  is the maximum achievable display intensity. The image function IMAGE from MATLAB was used for the color monitor display.

### 3. Results and Discussion

#### A. Wave-Band Selection for Two-Band Color-Mixing Binoculars

Figure 1 shows a plot of the minimum  $\Delta E$  values for all the possible wave-band combinations (90,000 wave-band pairs) for multitarget detection. Because the contour plot is symmetric about the diagonal, only the upper half of the plot is discussed here. Four areas of peak  $\Delta E$  values occur near the  $(\lambda_1, \lambda_2)$  wave-band pairs of (427 nm, 664 nm), (450 nm, 642 nm), (453 nm, 589 nm), and (531 nm, 618 nm), for which the  $\Delta E$  values are 4.35, 4.47, 4.34, and 3.76, respectively. Although the highest  $\Delta E$  values occur for the first two pairs, the relative luminous efficiency of the human eye is extremely low at these wavelengths, thus rendering these wave bands unsuitable for filter selection. The wave-band pair of (453 nm, 589 nm) has the next-highest  $\Delta E$  and thus is a potential filter

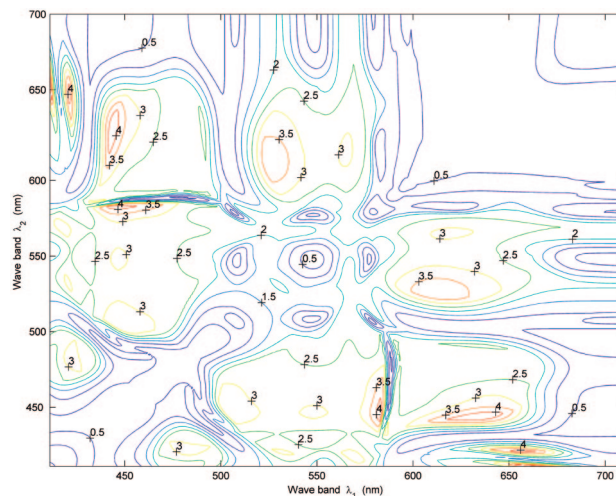


**Fig. 1. Contour plot of minimum color difference values  $\Delta E$  between wave-band pairs centered at  $\lambda_1$  and  $\lambda_2$  for multitarget detection.**

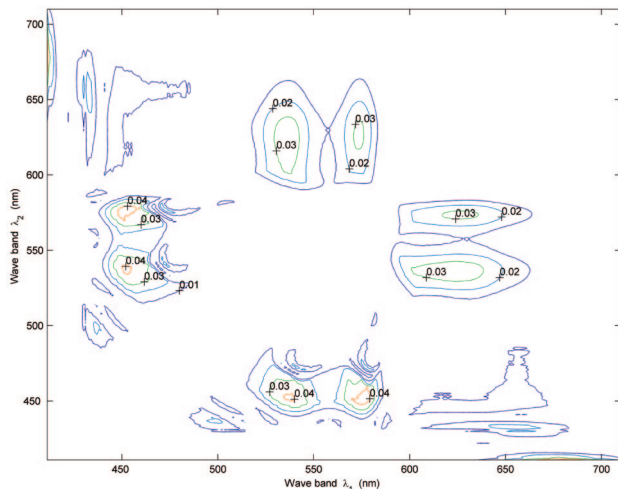
**Table 2. Wave-Band Pairs Selected with Color Difference Index  $\Delta E$  and Chromaticness Difference Index  $\Delta S'$**

Target Condition	$\Delta E$		$\Delta S'$	
	$\lambda_1$ (nm)	$\lambda_2$ (nm)	$\lambda_1$ (nm)	$\lambda_2$ (nm)
Multitarget	453	589	454	578
Single-target: wholesome	486	636	449	571
Single-target: air-sac	449	588	441	576
Single-target: cadaver	458	576	462	575
Single-target: IP	456	599	454	591
Single-target: septox	454	590	509	628
Single-target: tumor	434	512	431	501

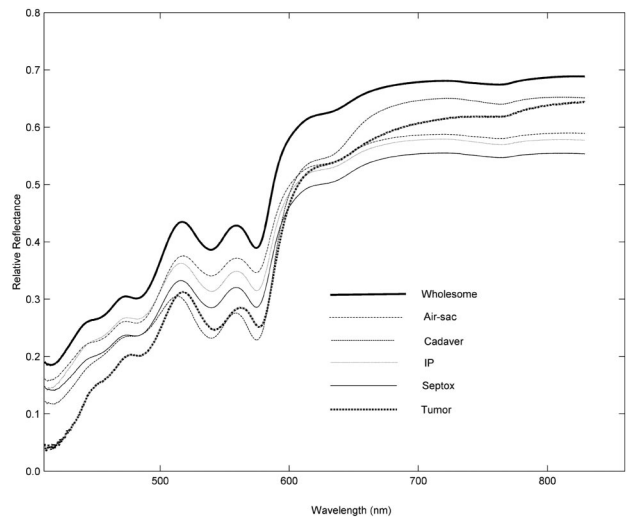
selection for multitarget detection. Table 2 shows the wave-band pairs for potential filter selection for single-target detection, which were also determined according to the maximum of minimum  $\Delta E$  values as described above.

Figure 2 shows a plot of the minimum  $\Delta S'$  values for all the possible wave-band combinations (90,000 wave-band pairs) for multitarget detection. Four areas of peak  $\Delta S'$  values occur near the  $(\lambda_1, \lambda_2)$  wave-band pairs of (454 nm, 578 nm) (452 nm, 537 nm), (624 nm, 538 nm), and (627 nm, 574 nm), for which the  $\Delta S'$  values are 0.0467, 0.0412, 0.0355, and 0.0320, respectively. The wave-band pair of (454 nm, 578 nm) has the highest  $\Delta S'$  value and is a potential selection for multitarget detection when the color differences are large enough. Table 2 shows the wave-band pairs for potential filter selection for single-target detection, which were also determined according to the maximum of minimum  $\Delta S'$  values as described above.

Figure 3 shows the average spectra of wholesome, air-sac, cadaver, IP, septox, and tumor chickens. The visible region contains more useful spectral features for differentiating between conditions than the NIR region. Myoglobin comprises 50%–80% of the meat



**Fig. 2. Contour plot of minimum chromaticness difference values  $\Delta S'$  between wave-band pairs centered at  $\lambda_1$  and  $\lambda_2$  for multitarget detection.**



**Fig. 3. Averaged spectra for wholesome, air-sac, cadaver, IP, septox, and tumor chickens.**

pigment mass.<sup>19,20</sup> For chicken meat, spectral features in the visible region are determined primarily by the relative amounts of three forms of myoglobin, i.e., deoxymyoglobin, metmyoglobin, and oxymyoglobin. The deoxymyoglobin and oxymyoglobin components coexist with metmyoglobin in both wholesome and unwholesome chicken meat. These three forms of myoglobin can interconvert and may degrade through oxygenation, oxidation, and reduction reactions when external processes such as cold storage or cooking are applied.<sup>12,21</sup> Bands associated with myoglobin include those in the areas of 430, 440, and 455 nm with deoxymyoglobin; 485, 495, and 505 nm with metmyoglobin; and 545, 560, and 575 nm with oxymyoglobin.<sup>12</sup> The potential wave-band pairs for single-target and multitarget detection, shown in Table 2, reflect some of these spectral regions known to show myoglobin-related changes correlated to wholesome and unwholesome chicken conditions.

Tables 3 and 4 show the  $\Delta E$  color differences calculated for the color mixing of the potential wave-band pairs for multitarget detection that were determined from peak areas selected from Figs. 1 and 2, (453 nm, 589 nm) and (454 nm, 578 nm), respectively. With the selection of either of these pairs for color appearance simulation, the color differences between the wholesome and five unwholesome carcass types are great enough to differentiate between the individual categories.

In general, wholesome and unwholesome chicken can be characterized by the relative amounts of these myoglobin forms, with wholesome chicken containing more oxymyoglobin and deoxymyoglobin and unwholesome chicken containing more metmyoglobin.<sup>21</sup> Consequently, in selecting wave-band pairs for color appearance simulation from the potential pairs listed in Table 2, preference was given to those pairs more closely associated with the deoxymyoglobin, metmyoglobin, and oxymyoglobin wave bands. Wave-band

**Table 3. Color Difference  $\Delta E$  between Sample Categories with  $\lambda_1 = 453 \text{ nm}$  and  $\lambda_2 = 589 \text{ nm}$**

	Wholesome	Air-sac	Cadaver	IP	Septox	Tumor
Wholesome	0.0	5.56	16.5	12.5	10.5	11.7
Air-sac		0.0	11.2	7.82	5.03	9.46
Cadaver			0.0	4.68	6.36	16.2
IP				0.0	4.42	15.2
Septicemia					0.0	10.8
Tumor						0.0

**Table 4. Color Difference  $\Delta E$  between Sample Categories with  $\lambda_1 = 454 \text{ nm}$  and  $\lambda_2 = 578 \text{ nm}$**

	Wholesome	Air-sac	Cadaver	IP	Septox	Tumor
Wholesome	0.0	3.57	26.5	10.7	11.0	11.9
Air-sac		0.0	25.9	10.4	9.66	8.36
Cadaver			0.0	15.8	16.4	24.6
IP				0.0	2.97	12.2
Septicemia					0.0	9.60
Tumor						0.0

pairs selected for color appearance simulation are shown in Table 5.

**B. Simulation of Color Appearance**

For multitarget detection using the (454 nm, 578 nm) wave-band pair, the color chart produced by the color appearance simulation is shown in Fig. 4. Against the medium-gray background ( $\rho = 0.2$ ), all six simulated chicken condition colors are easily differentiated, with the wholesome color contrasting the most against the background. Among the six conditions, the cadaver and tumor colors are the most distinct from the other conditions, whereas the IP and septox colors are the most similar and thus more difficult to distinguish from each other. Table 6 shows the device-independent appearance correlates for the multitarget simulation. Examining these values, it is evident that the lightness ( $J$ ) is the greatest for wholesome chicken, which accounts for the most significant contrast against the background. The difference in hue angle ( $h$ ) between cadaver and each of the other five conditions is always at least  $115^\circ$ , and saturation is greatest for the tumor condition. Both of these conditions have relatively low lightness values. These factors render the cadaver and the tumor colors the most distinct from the others. All three appearance correlates are similar between IP and septox.

**Table 5. Wave-Band Pairs Selected for Color Appearance Simulation**

Target Condition	$\lambda_1$ (nm)	$\lambda_2$ (nm)
Multitarget	454	578
Single-target: wholesome	449	571
Single-target: air-sac	441	576
Single-target: cadaver	458	576
Single-target: IP	454	591
Single-target: septox	454	590
Single-target: tumor	431	501

The purpose of single-target detection is to identify the target chicken condition. The color charts for single-target detection are shown in Figs. 5–10. Here, for brevity, only appearance correlates for the wholesome target are shown in Table 7. Using the wave-band pair (449 nm, 471 nm) for single-target detection of wholesome chickens (Fig. 5), the wholesome color is clearly lighter than all the other conditions, with a lightness of 56.27 compared to 51.83 for air-sac and 40.09 for cadaver. Using the wave-band pair (441 nm, 576 nm) for single-target detection of air-sac (Fig. 6), air-sac appears to be well differentiated from the other conditions. In comparison to air-sac, wholesome has greater lightness, cadaver and tumor are both significantly different in hue, and IP and septox have similar lightness but much lower saturation. Using the wave-band pair (458 nm, 576 nm) for single-target detection of cadaver (Fig. 7), cadaver is clearly distinct from all



**Fig. 4. Color chart for multitarget detection using the wave-band pair (454 nm, 578 nm).**

**Table 6. Parameters Calculated from CIECAM97s Model at Wavelength Pair (454 nm, 578 nm)**

	Wholesome	Air-sac	Cadaver	IP	Septox	Tumor
Lightness, $J$	56.18	51.88	39.58	48.68	45.81	41.84
Hue angle, $h$	95.68	100.10	319.38	74.50	88.24	105.71
Saturation, $s$	14.82	19.04	15.75	7.27	10.35	27.69

**Table 7. Parameters Calculated from CIECAM97s Model at Wavelength Pair (449 nm, 571 nm)**

	Wholesome	Air-sac	Cadaver	IP	Septox	Tumor
Lightness, $J$	56.27	51.83	40.09	49.00	46.00	43.27
Hue angle, $h$	127.4	125.5	178.3	132.6	129.5	121.8
Saturation, $s$	27.81	31.45	8.486	20.24	24.03	49.71

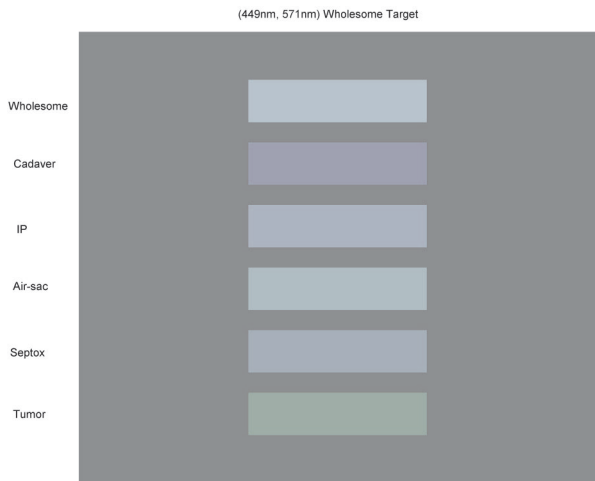


Fig. 5. Color chart for single-target wholesome detection using the wave-band pair (449 nm, 571 nm).



Fig. 7. Color chart for single-target cadaver detection using the wave-band pair (458 nm, 576 nm).

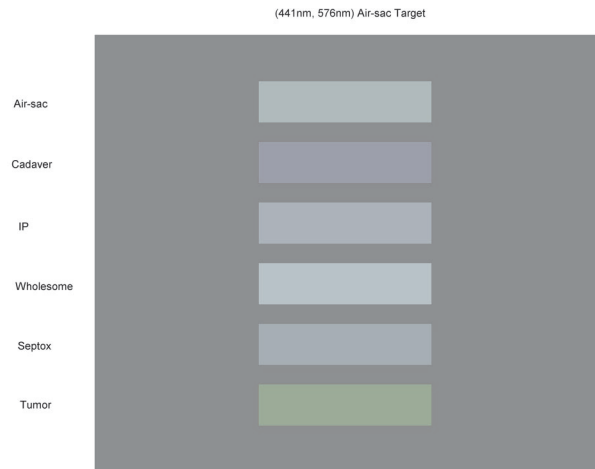


Fig. 6. Color chart for single-target air-sac detection using the wave-band pair (441 nm, 576 nm).



Fig. 8. Color chart for single-target IP detection using the wave-band pair (454 nm, 591 nm).

five other conditions due to significant angle and saturation. Using the wave-band pair (454 nm, 591 nm) for single-target detection of IP (Fig. 8), IP is not as easily differentiated from the other conditions, except wholesome and tumor, which show

greater lightness and greater saturation, respectively. Using the wave-band pair (454 nm, 590 nm) for single-target detection of septox (Fig. 9), septox is similar to air-sac and cadaver but can be distinguished by lightness from wholesome and by satu-

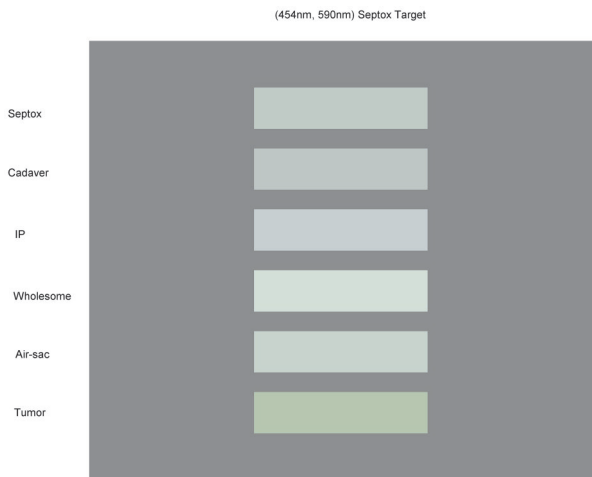


Fig. 9. Color chart for single-target septox detection using the wave-band pair (454 nm, 590 nm).



Fig. 10. Color chart for single-target tumor detection using the wave-band pair (431 nm, 501 nm).

ration from tumor. Using the wave-band pair (431 nm, 501 nm) for single-target detection of tumor (Fig. 10), tumor is easily identified by its hue angle.

In a practical processing plant situation, chicken carcasses are moving across an inspector's field of view. A color chart similar to those in Figs. 4–10, marked with the standard color appearance of target carcass conditions, could be placed just behind the moving birds for direct comparison of color. This would aid inspectors using color-mixing binoculars for identification of specific carcass conditions.

#### 4. Summary and Conclusion

From wholesome and unwholesome chicken spectra measured in the visible spectrum region, a search for 10 nm wave-band pairs has been conducted with color difference and chromaticness difference indices for potential pairs to use in the selection of binocular filters for single-target and multitarget detection of

chicken conditions. For multitarget detection, the wave-band pair (454 nm, 578 nm) was selected. For single-target detection of wholesome, air-sac, cadaver, IP, septox, and tumor conditions, the selected wave-band pairs were (449 nm, 571 nm), (441 nm, 576 nm), (458 nm, 576 nm), (454 nm, 591 nm), (454 nm, 590 nm), and (431 nm, 501 nm), respectively. The CIECAM97s color appearance model was used to simulate the use of two-band color-mixing binoculars for the detection of wholesome and unwholesome chicken conditions.

All six chicken conditions could be distinguished with the wave-band pair (454 nm, 578 nm) selected for multitarget detection. The selected single-target wave-band pairs (449 nm, 571 nm), (441 nm, 576 nm), (458 nm, 576 nm), and (431 nm, 501 nm) were able to identify wholesome, air-sac, cadaver, and tumor, respectively, without difficulty. The single-target wave-band pairs (454 nm, 591 nm) and (454 nm, 590 nm) for IP and septox, respectively, were able to easily differentiate the target conditions from wholesome and tumor but could not identify the target conditions from the remaining unwholesome conditions.

Two-color-mixing binoculars thus show potential for practical use in a processing plant environment. The inspection process could be easily enhanced by inspectors using such a simple and compact optical device. This will directly affect small-scale meat and poultry processors in terms of improved efficacy of the HACCP program.

The authors thank Xuemei Zhang, Agilent Technologies Inc.; Michael D'Zmura, University of California, Irvine; and David R. Wyble, Munsell Color Science Laboratory, Rochester Institute of Technology, for their kind suggestions, and Diane E. Chan for her assistance in conducting the experiment for this study and preparing this manuscript. Mention of a product or specific equipment does not constitute a guarantee or warranty by the U.S. Department of Agriculture and does not imply its approval to the exclusion of other products that may also be suitable.

#### References

1. USDA, FSIS, *USDA Poultry Inspection Flier* (USDA, FSIS, 1989).
2. B. P. Dey, Y. R. Chen, C. Hsieh, and D. E. Chan, "Detection of septicemia in chicken livers by spectroscopy," *Poult. Sci.* **82**, 199–206 (2003).
3. USDA, FSIS, *Pathogen Reduction, Hazard Analysis and Critical Control Point (HACCP) Systems. Final Rule. Federal Register 61:28805–38855* (USDA, FSIS, 1994).
4. R. Lu and Y. R. Chen, "Hyperspectral imaging for safety inspection of food and agricultural products," in *Pathogen Detection and Remediation for Safe Eating*, Proc. SPIE **3544**, 121–133 (1998).
5. Y. R. Chen, W. R. Hruschka, and H. Early, "A chicken carcass inspection system using visible/near-infrared reflectance: in plant trials," *J. Food Process Eng.* **23**, 89–99 (2000).
6. Y. R. Chen, "Classifying diseased poultry carcasses by visible and near-IR reflectance spectroscopy," in *Optics in Agriculture and Forestry*, J. A. DeShazer and G. E. Meyer, eds., Proc. SPIE **1836**, 44–55 (1992).

7. B. Park, Y. R. Chen, and M. Nguyen, "Multi-spectral image analysis using neural network algorithm for inspection of poultry carcasses," *J. Agric. Eng. Res.* **69**, 351–363 (1998).
8. K. Chao, Y. R. Chen, W. R. Hruschka, and F. B. Gwozdz, "On-line inspection of poultry carcasses by dual-camera system," *J. Food Eng.* **51**, 185–192 (2002).
9. K. Chao, P. M. Mehl, and Y. R. Chen, "Use of hyper- and multi-spectral imaging for detection of chicken skin tumors," *Appl. Eng. Agric.* **18**, 113–119 (2002).
10. K. Chao, Y. R. Chen, and D. E. Chan, "Analysis of Vis/NIR spectral variations of wholesome, septicemia, and cadaver chicken samples," *Appl. Eng. Agric.* **19**, 453–458 (2003).
11. F. Ding, Y. R. Chen, K. Chao, and D. E. Chan, "Two-color mixing for classifying agricultural products for safety and quality," *Appl. Opt.* (to be published).
12. Y. Liu and Y. R. Chen, "Analysis of visible reflectance spectra of stored, cooked and diseased chicken meats," *Meat Sci.* **58**, 395–401 (2001).
13. R. S. Berns, *Bilmeyer and Saltzman's Principles of Color Technology* (Wiley, 2000).
14. G. Wyszecki and W. S. Stiles, *Color Science: Concepts and Methods, Quantitative Data and Formulas* (Wiley, 1982).
15. M. D. Fairchild, "A revision of CIECAM97s for practical applications," <http://www.cis.rit.edu/people/faculty/fairchild/PDFs/PAP10.pdf>.
16. CIE TC1-34, "The CIE 1997 Interim Colour Appearance Model (Simple Version), CIECAM97s April 1998," [http://www.cis.rit.edu/people/faculty/fairchild/PDFs/CIECAM97s\\_TC\\_Draft.pdf](http://www.cis.rit.edu/people/faculty/fairchild/PDFs/CIECAM97s_TC_Draft.pdf).
17. M. D. Fairchild, "Considering the surround in device-independent color imaging," *Color Res. Appl.* **20**, 352–363 (1995).
18. L. J. Barco, J. A. Diaz, J. R. Jimenez, and M. Rubino, "Considerations on the calibration of color displays assuming constant channel chromaticity," *Color Res. Appl.* **20**, 377–387 (1995).
19. D. M. Kinsman, A. W. Kotula, and B. C. Breidemeststein, *Muscle Foods* (Chapman & Hall, 1994).
20. H. J. Swatland, "A review of meat spectrophotometry (300 to 800 nm)," *J. Can. Inst. Food Sci. Technol.* **22**, 390–402 (1989).
21. Y. Liu, Y. R. Chen, and Y. Ozaki, "Characterization of visible spectral intensity variations of wholesome and unwholesome chicken meats with two-dimensional correlation spectroscopy," *Appl. Spectrosc.* **54**, 587–594 (2000).